Langmuir

Article

pubs.acs.org/Langmuir

18-Crown-6−Sodium Cholate Complex: Thermochemistry, Structure, and Stability

Tea Mihelj,*,† Vlasta Tomašić,*,† and Nikola Biliškov‡

†Department of Physical Chemistry and ‡Division of Materials Chemistry, Ruđer Bošković Institute, POB 180, HR-10002 Zagreb, Croatia

Supporting Information

ABSTRACT: 18-Crown-6, one of the most relevant crown ethers, and sodium cholate, a steroidal surfactant classified as a natural bile salt, are components of a novel, synthesized coordination complex: 18-crown-6−sodium cholate (18C6·NaCh). Like crown ethers, bile salts act as building blocks in supramolecular chemistry to design new functionalized materials with a desired structure and properties. In order to obtain thermal behavior of this 1:1 coordination complex, thermogravimetry and differential thermal analysis were used, as well as microscopic observations and differential scanning calorimetry. Temperature dependent infrared (IR) spectroscopy gave a detailed view into phase transitions. The structures during thermal treatment were observed with powder X-ray diffraction, and molecular models of the phases were made. Hard, glassy, colorless compound 18C6·NaCh goes through crystalline−crystalline polymorphic phase transitions at higher temperatures. The room temperature phase is indexed to a triclinic lattice, while in the high temperature phases molecules take randomly one of the two different configurations in the unit cell, resulting in the 2-fold symmetry. The formation of cholesteric liquid crystalline phase occurs simultaneously with partial decomposition, followed by the isotropization with simultaneous and complete decomposition at much higher temperature, as obtained by IR. The results provide valuable information about the relationship between molecular structure, thermal properties, and stability of the complex, indicating the importance of an appropriate choice of cation, amphiphilic, and crown ether unit in order to synthesize compounds with desired behavior.

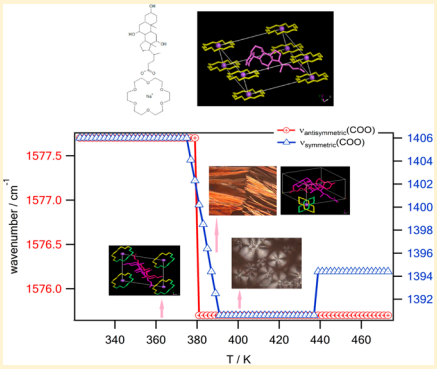

1. INTRODUCTION

Crown ethers constitute one of the most prominent molecules in host−guest chemistry, often called the simplest benchmark substrates resembling the general features of key-pocket inclusion complexes.[1] Among the most salient properties of crown ethers stands their specific binding and solvation of cationic species, alkali, alkaline-earth, transition-metal, and ammonium cations,[2−6] which makes them a perfect and valuable tool in organic synthesis. These macrocyclic polyethers are known as neutral complexing agents, with specific selectivity as the result of their cavity size that adopts cations of comparable ionic radii and the capability of the cyclic ether backbone to build a coordination shell, optimizing the interaction of its electron donor oxygen sites with the cation.[7−9] The number and type of donor atoms, conformational flexibility for most effective coordination, as well as the size and form of the coordinated guest and charge density dictate different binding activity, as well as preorganization by means of symmetric and chiral arrangements and the solvent effect.[4,8,10,11] Consequently, these "ionophore-model systems" are very attractive to chemists and applicable in many areas; from biological mimics, and models of biological receptors,[12] to recovery, removal or selective complexation and transport of species,[13] usage in environmental,[14,15] as well as pharmaceutical[16,17] applications. Moreover, they have been used as building blocks for a broad range of modern materials,[10,18,19] chromatographic agents,[20,21] and so forth. Alkali metal elements have an important role in biological processes, primarily as bulk electrolytes that stabilize surface charges on proteins and nucleic acids,[22] and also play unique structural role in biological systems.[23,24] Crown-ligands with alkali metal elements make coordination compounds based on electrostatic interaction through ion-dipole attractions,[25] useful for simulations of properties and behavior of natural substances.

Cholic acid is a steroidal surfactant compound classified as a natural bile acid. The literature describes a vast amount of pharmacological applications of bile acids and their derivatives, including the use in treatment of their deficiency, dissolution of cholesterol gallstones,[26] and antiviral[27] and antifungal properties.[28] Like crown ethers, bile acids act as building blocks in supramolecular chemistry to design new antibiotics,[29] cationic or anionic receptors,[30,31] templates, scaffolds, or ionic channels.[32,33] Some cholic acid based macrocyclic compounds are cholaphanes usually used as transmembrane anion carriers,[34] cyclocholates used in host−guest chemistry or molecular recognition studies,[35] as well as bile acid based chiral dendrons of nanometric dimensions,[36] or molecular boxes.[37] It is already known

Received: March 26, 2014
Revised: May 7, 2014
Published: May 7, 2014

dx.doi.org/10.1021/la501155s | Langmuir 2014, 30, 6274−6285

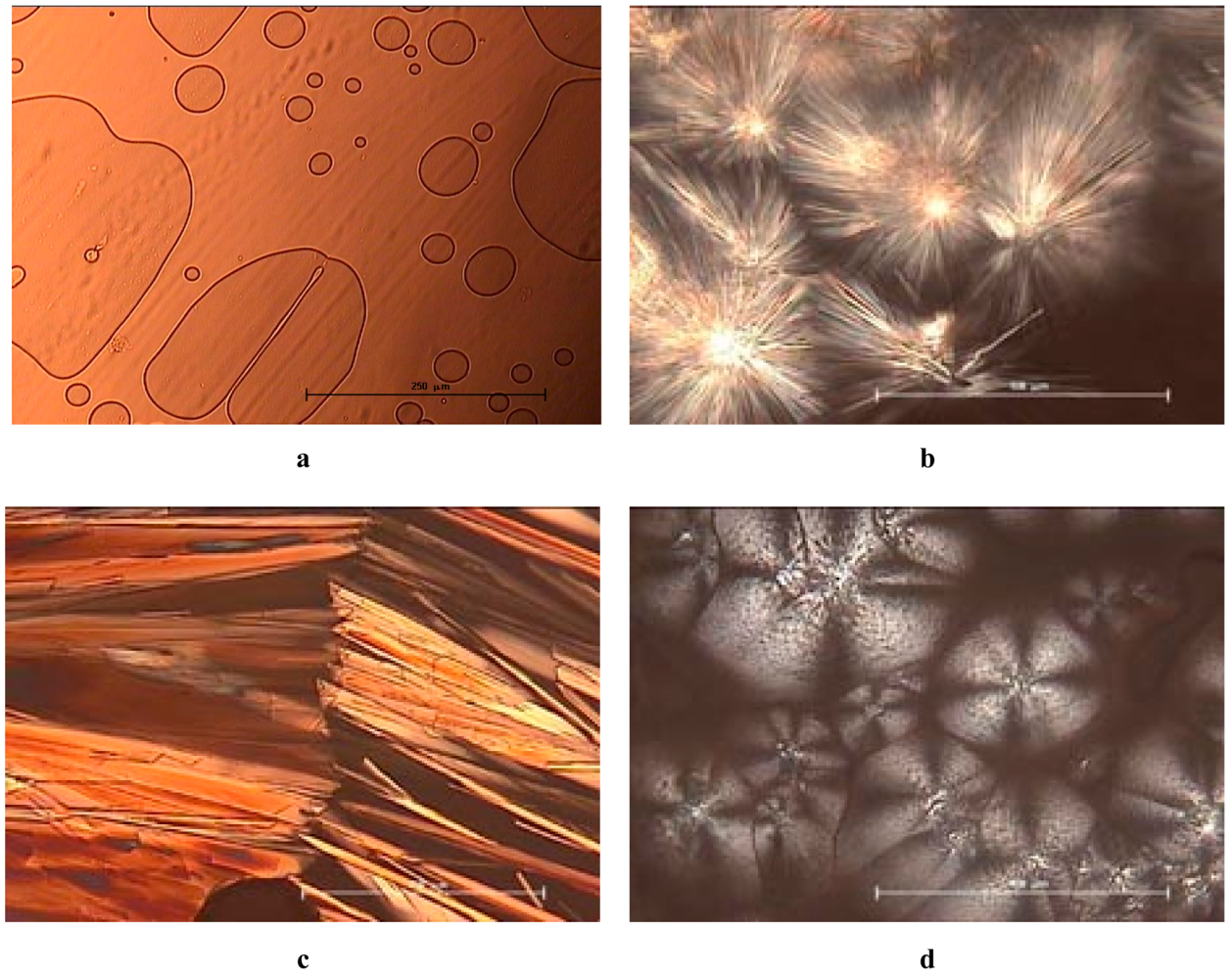

Figure 1. Micrographs of the characteristic textures for examined complex taken in the heating cycle via optical microscope, under phase contrast (a) and crossed polarizers (b–d): RT (a); 355 K (b); 386 K (c), and 400 K (d). Bar represents 250 μm (a and c) and 100 μm (b and d).

that cholic acid forms inclusion crystals with various guest compounds.

Attempts to form inclusion crystals of cholic acid with various guest compounds have revealed a variety of molecular assemblies, with the hydrogen bonding directly involved in the structure of bile acid crystals and forming different network patterns: from two-dimensional sheets[38,39] to three-dimensional host frameworks, making cumulated channel-type bilayers, accompanied by guest responsive transformations of crystal structure, and variable guest-dependent polymorphism.[40,41] Host–guest compounds of cholic acid with *n*-alkylammonia revealed two types of bilayer-like structures; in 1:1 complexes, guests are included in the hydrophobic zones between those layers in a kind of sandwich-type structure, while in 2:1 compound bilayers cross and form one-dimensional hydrophobic channels into which guest molecules are included.[42] Besides crossing structures with cagelike cavities and bilayered structures with channellike cavities, the honeycomb structure with hexagonal channels is also representative crystal structure of cholic acid drivatives.[43] In general, more than 13 kinds of host frameworks, differing in volume, shape, polarity, and chirality of guests, have been found so far.[38,39] Diversity is the result of the hierarchical structure in steroids, based on characteristic bimolecular and helical 2_1 screw assemblies,[44] retained by the hydrogen bonding network of the three hydroxyl groups in the steroidal skeleton, and building bundles. Moreover, it is the result of the steroidal skeleton asymmetry, facial amphiphilicity of molecules,[40] type of guest components,[42] and various combination of hydrogen-bonding arrangements. In principle, the bile salt molecules possess information, expressed through their molecular architecture.

Complexes formed between crown ether compounds and surfactants are less explored, especially in terms of thermochemical studies. A lot of studies conducted on crown ether complexes provided information about thermotropic mesomorphism during thermal treatment, from hexagonal columnar mesophases in complexes with 18-crown-6 drivatives,[45,46] to cholesteric liquid crystalline behavior for cholesteryl esters bearing 16-membered crown ethers.[47] Complexes with crown ethers containing aza, thio units or other heteroatoms have also shown rich thermal behavior with polymorphism and liquid crystal formation.[48−51] This Article comprises structural and thermochemical study of a novel 18-crown-6 (18C6) complex with sodium cholate. X-ray diffraction techniques are one of the most reliable methods to solve the structure. Due to the complex nature of steroidal compounds and thus more tedious procedures, single X-ray diffraction has been more often used in determination of molecular arrangement in crystals,[39,42,52−54] rather than powder X-ray diffraction. In this study, the structure of 18C6–sodium cholate complex is completely characterized with temperature dependent powder X-ray diffraction technique. Besides thermogravimetry, microscopic observations, and

dx.doi.org/10.1021/la501155s | *Langmuir* 2014, 30, 6274−6285

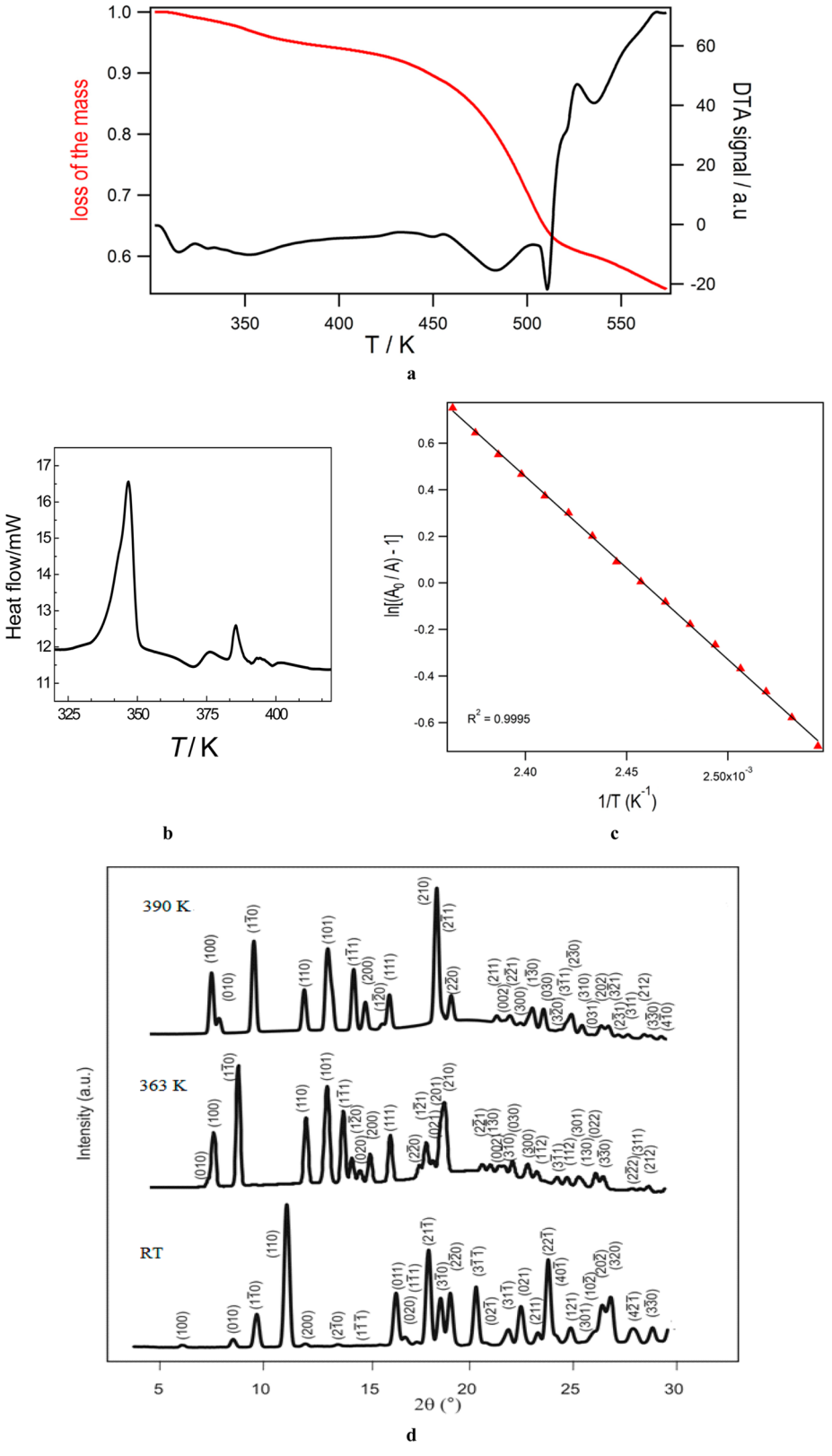

Figure 2. Representative thermogram (red line) and DTA result (black line) (a); DSC thermogram (b) for examined complex 18C6·NaCh; and thermodynamics of crown 18C6 decomplexation from 18C6·NaCh complex given by IR (c). PXRD diffractograms of 18C6·NaCh at different temperatures, chosen and indexed due to obtained thermal changes at characteristic temperatures (d).

differential scanning calorimetry, infrared spectroscopy in a wide temperature range was used. It was recently shown by Zimmermann and Baranović[55] that phase transitions can be detected by rapid and simple analysis of absolute variations of a baseline in a temperature-dependent mid-infrared transmittance spectra. The method is based exclusively on changes in optical properties of the material under investigation. Thus, some phase transitions, overlooked by more commonly used methods,

dx.doi.org/10.1021/la501155s | *Langmuir* 2014, 30, 6274−6285

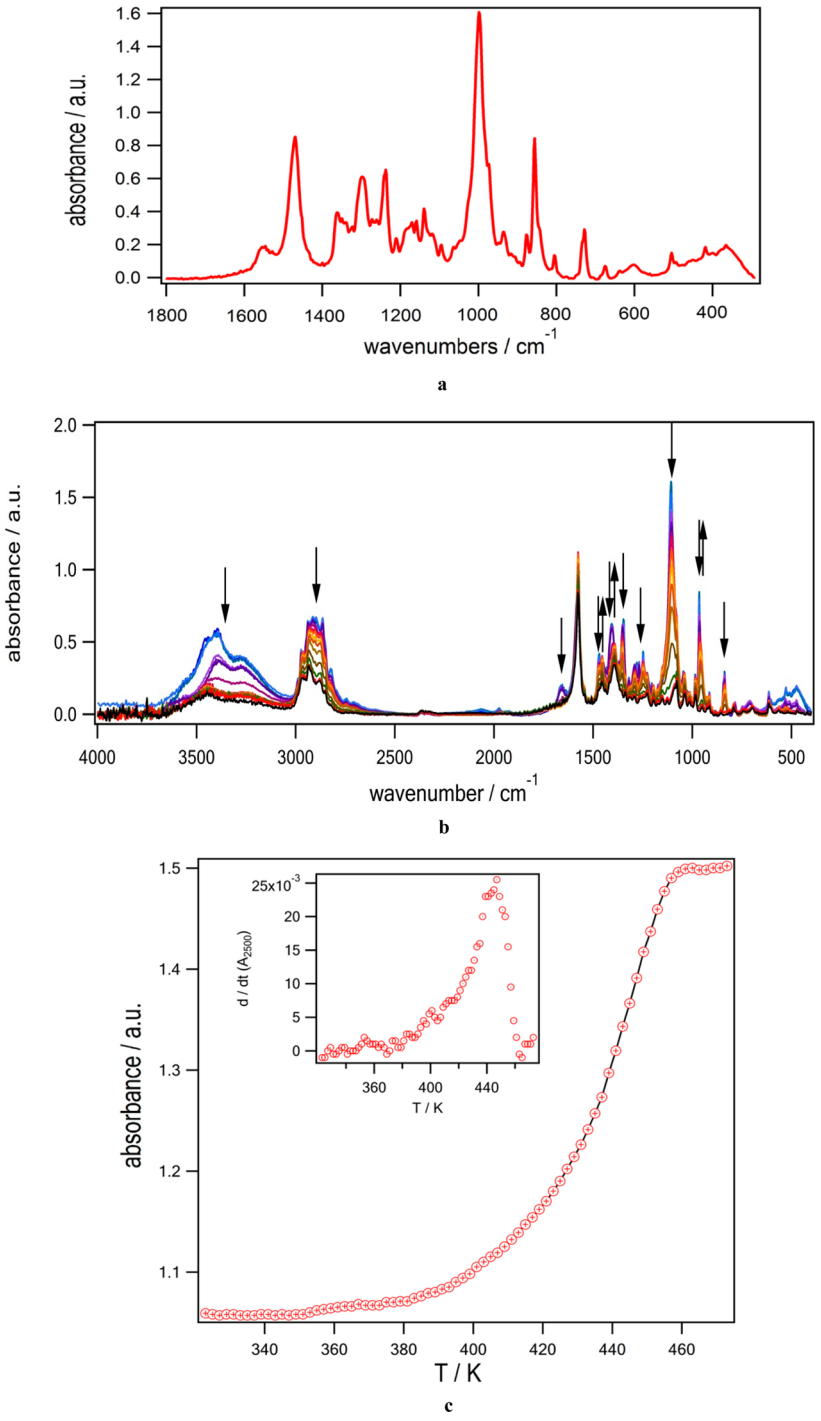

Figure 3. Infrared spectra of 18C6·NaCh complex at RT in the 1900−400 cm^{-1} region (a). Baseline corrected variable-temperature infrared spectra in the 323−473 K temperature interval (b), and temperature dependence of the baseline absorption (c). Inset shows the first derivative of the curve for the purposes of determination of the transition temperature. A detailed view of spectra with the most prominent changes at defined temperatures is seen in Figure S1 (Supporting Information).

become readily evident by IR spectroscopy, as seen in our recent publications.[56,57] Further advantage of temperature-dependent IR spectroscopy lies in the fact that it provides an elegant link between macroscopic and microscopic properties. In other words, it does not only detect phase transitions, but the variations in the fingerprint region of the recorded spectra reflect the changes at molecular level, which are manifested at macroscopic level as phase transitions. The results given in this study provide valuable information about the relationship between molecular structure, thermal properties, and stability of the complex, indicating the importance of an appropriate choice of cation and crown ether unit to synthesize compounds with eligible behavior. Such experiments widen the research field of ion complexation and supramolecular chemistry to make new, functionalized materials with a desired structure and properties.

2. EXPERIMENTAL SECTION

Materials, Complex Preparation, and Identification. 18-Crown-6 ether, that is, 1,4,7,10,13,16-hexaoxacyclooctadecane (18C6, $C_{12}H_{24}O_6$, M_w = 264.32 g mol^{-1}), and sodium cholate hydrate, that is,

dx.doi.org/10.1021/la501155s | Langmuir 2014, 30, 6274−6285

3α,7α,12α-trihydroxy-5β-cholanic-acid sodium salt (NaCh, $C_{24}H_{39}O_5Na$, M_w = 430.60 g mol^{-1}; Sigma Ultra, min. 99%), were obtained from Sigma-Aldrich and used without further purification for the preparation of the complex.

18-Crown-6- sodium cholate complex (18C6·NaCh) was prepared by high temperature mixing of equimolar aqueous solutions of both components. After aging (few days at room temperature), during which water spontaneously evaporated, the sample was dried under vacuum at room temperature (RT) until constant mass was obtained, and then the sample was stored protected from moisture and light before use. The precipitated compound was waxy and after being vacuum-dried and was glassy, colorless, and transparent.

The identification of complex was performed by elemental analysis (PerkinElmer Analyzer PE 2400 Series 2). Elemental analysis expressed as mass fraction in percent confirmed that the complex is 1:1 charge ratio adduct: $C_{36}H_{63}O_{11}Na$, M_w = 694.92 g mol^{-1}. Found: C, 62.30; H, 9.20; requires C, 62.23; H, 9.14%. It was also characterized by NMR (Avance 600 Bruker with supraconducting magnet, 14 T field strength, frequency range 24−600 MHz and temperature range 223−373 K) according to the following designation:

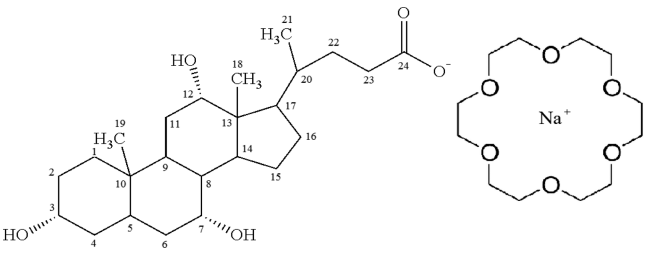

^{13}C NMR (150 MHz, D_2O, 323.15 K) σ/ppm: 73.45 (C12), 71.91 (C3), 69.85 (CH_2 (crown)), 68.62 (C7), 47.03 (C17), 46.48 (C13), 41.85 (C5), 41.48 (C14), 39.61 (C8), 38.82 (C4), 35.72 (C20), 35.17 (C23), 34.67 (C10), 34.21 (C6), 32.52 (C22), 29.65 (C2), 28.02 (C11), 27.48 (C16), 26.73 (C9), 23.21 (C15), 22.38 (C19), 17.14 (C21), 12.42 (C18).

^{1}H NMR (600 MHz, D_2O, 323.15 K) σ/ppm: 4.76 (1H, s, OH (C3)), 4.34 (1H, s br, OH (C12)), 4.18 (1H, s br, OH (C7)), 4.12−3.96 (24H, s, CH_2 (crown)), 3.96 (1H, s, CH (C7)), 3.81−3.75 (1H, m, J = 4.137 CH (C3)), 2.55 (1H, m, CH_2 (C23)), 2.47−2.34 (3H, m, CH_2 (C4, C23), CH (C9)), 2.29−2.21 (2H, m, CH_2 (C22, C6), 2.17−2.09 (2H, m, CH_2 (C4), CH (C14)), 2.06−1.84 (10 H, m, CH_2 (C22, C1, C15, C2, C11, C6, C16), CH (C17, C8)), 1.74−1.58 (5H, m, CH_2 (C2, C16), CH (C20, C5)), 1.29 (3H, d, J = 6.44, CH_3 (C21)), 1.21 (3H, s, CH_3 (C19)), 1.01(3H, s, CH_3 (C18)).

Measurements. *Thermogravimetry (TG).* The loss of weight due to the heating was measured by TG, with a Shimatzu DTG-60H instrument. The sample was heated from RT to 573 K at the heating rate of 5 K min^{-1} in synthetic airflow of 50 mL min^{-1}. The temperature range for thermal analysis of the sample was determined by examination of TG and DTA (differential thermal analysis) curves.

Differential Scanning Calorimetry (DSC). DSC was carried out with a PerkinElmer Pyris Diamond DSC calorimeter in N_2 atmosphere equipped with a model PerkinElmer 2P intracooler in N_2 atmosphere, at the rate of 2 K min^{-1}. Temperature and enthalpy calibrations were performed using high purity standards (*n*-decane and indium). The transition enthalpy, ΔH/kJ mol^{-1}, was determined from the peak area of the DSC thermogram; and the corresponding entropy change, ΔS/J mol^{-1} K^{-1}, was calculated using the maximal transition temperature. All results are mean values of several independent measurements carried out on different samples of the same compound, taken from the first heating and cooling run.

Microscopy. Textures were examined with a Leica DMLS polarized optical light microscope, equipped with a Mettler FP 82 hot stage, and a Sony digital color video camera (SSC-DC58AP).

Infrared (IR) Spectroscopy. IR transmission spectra of the solid samples were recorded at 4 cm^{-1} resolution in KBr pellets on an ABB Bomem MB102 single-beam FT-IR spectrometer with CsI optics, DTGS detector. The KBr sample pellets were prepared by mixing ∼2 mg of the individual sample with 100 mg of KBr with a pestle and mortar made of agate. The use of KBr as matrix allows the usable spectral range of 4000−300 cm^{-1}. Each spectrum represents an average of 100 Fourier-transformed interferograms. A Specac 3000 series high-stability temperature controller with a water cooled heating jacket was used to measure the spectra within the temperature range from RT up to 523 K under atmospheric conditions and at heating rate of 2 K min^{-1} and 2 K steps. In variable-temperature infrared spectroscopy, heat is used as an outside perturbation, while the consequent changes in infrared spectra reflect the rearrangement of the sample on molecular level. It should be remarked that experimental setup, that is, KBr pellets transmission technique, constitutes a thermodynamically open system. Thus, it allows free diffusion of the gaseous products, which arise due to the heating of the sample. Each single-beam spectrum collected in a temperature run for individual sample was ratioed to the single-beam spectrum of the sample-free setup (the reference spectrum) recorded immediately before starting the temperature-dependent measurements.

Powder X-ray (PXRD) Diffraction. PXRD diffractograms were recorded using a rotating anode copper source (λ/Å = 1.54) and a MAR345 image plate detector. The powder sample was put in a glass capillary, and its temperature was controlled using a cryojet system (Oxford Instrument). The 2D diffraction patterns were converted to $I-2\theta$ curves by radial average.

Thermodynamics of the 18C6-Crown Decomplexation. Thermodynamics of the 18C6-crown decomplexation process was considered by infrared spectroscopy. Since decomplexed 18C6 crown is free to diffuse from the system, decomplexation is determined by equilibrium constant defined as

$$K = \frac{[\mathrm{MA}]}{[\mathrm{18C6{-}MA}]} \tag{1}$$

where the 18C6−MA and MA state for complexed and decomplexed salt of M = sodium (Na) and anion A = cholate (Ch), respectively. The amount of the produced MA is given by

$$[\mathrm{MA}] = c_0(\mathrm{18C6{-}MA}) - [\mathrm{18C6{-}MA}] \tag{2}$$

Since the experimental conditions allow free diffusion of the decomplexed 18C6 crown from the system, the expression for equilibrium constant is simplified to eq 3:

$$K = \frac{c_0(\mathrm{18C6{-}MA}) - [\mathrm{18C6{-}MA}]}{[\mathrm{18C6{-}MA}]} \tag{3}$$

Obviously, at room temperature, [18C6−MA] = c_0 (18C6 − MA), while at the end of decomplexation [18C6−MA] = 0 mol dm^{-3}. In terms of spectroscopic observables, the equilibrium constant is

$$K = \frac{A_0(\mathrm{18C6{-}MA})}{A(\mathrm{18C6{-}MA})} - 1 \tag{4}$$

where A_0 (18C6−MA) is absorbance of the band due to the 18C6−MA complex at 353 K, that is, when the sample is dehydrated. Now, combining the expression for equilibrium constant 4 with general expression for temperature dependence of equilibrium constant 5:

$$\ln K(T) = -\frac{\Delta H}{kT} + \frac{\Delta S}{k} \tag{5}$$

we obtain eq 6:

$$\ln\left[\frac{A_0(\mathrm{18C6{-}MA})}{A(\mathrm{18C6{-}MA})} - 1\right] = -\frac{\Delta H}{kT} + \frac{\Delta S}{k} \tag{6}$$

Therefore, enthalpy and entropy changes due to the decomplexation are readily obtained from the absorbance measurement of complexed and decomplexed sodium salt.

dx.doi.org/10.1021/la501155s | Langmuir 2014, 30, 6274−6285

3. RESULTS AND DISCUSSION

Solid-State Phase Transitions. Formation of solid 1:1 complex 18-crown-6-sodium cholate (18C6·NaCh) is accomplished through the equilibrium defined as

$$Na^+Ch^- + 18C6 \rightleftharpoons 18C6{\cdot}Na^+{\cdot}Ch^-$$

It is a hard, glassy, colorless and transparent compound (Figure 1a), which becomes crystalline by complete dehydration (Figure 1b) at cca. 355 K, as evident from TG, DSC, and temperature-dependent IR spectroscopy (Figures 2a,b and 3a,c). TG shows that the water contributes by 5% in the mass of the sample, which means that 2 water molecules bind to every 18C6·NaCh molecule. A prominent DSC endothermic peak (Table 1)

Table 1. Transition Temperatures, T/K, Enthalpies, ΔH/kJ mol^{-1}, and Entropies, ΔS/J mol^{-1} K^{-1}, during Heating and Cooling Cycles Given by DSC Measurements for 18C6·NaCh Complex, Together with the Parameters for Irreversible Decomplexation (italic text) of Crown 18C6 from Synthesized Compound, Calculated from the Absorbance Measurement of Complexed and Decomplexed Sodium Salt

heating		
T/K	ΔH/kJ mol^{-1}	ΔS/J mol^{-1} K^{-1}
346.8	27.0	77.9
380.6	2.4	6.2
410.2	0.5	1.2
445.0	*65.3*	*160.4*

indicates moderate O−H···O type hydrogen bonding. The most important functional groups assigned to spectral features at RT are presented in Figure 3a and Table 2. A slight rise of infrared baseline absorption at 353 K is well correlated with decrease of the mass, as observed by TG. Thus, it indicates dehydration of the sample. In this temperature region, IR spectra suffer the most prominent change in the 3700−3180 cm^{-1} range, attributed to hydrogen bonded water symmetric and antisymmetric OH stretching oscillators, but also to OH groups of cholate anion. Thus, this region was considered in more detail, and is explained in the Supporting Information (Figure S1). Comparison with TG and DSC data shows that dehydration occurs as two-step process, of which the first ends at 360 K. This corresponds well to behavior of the features due to the 18C6 moiety (Figure 4a and b). The step of dehydration is mainly due to water which is hydrogen bonded to 18C6 crown moiety. This explains the steep decrease of the intensity of the bands corresponding to characteristic ether ν(C−O−C) band at 964 cm^{-1} (Figure 4b), caused by the decrease in electron density on oxygen atoms of 18C6.

After that, another step occurs between 370 and 390 K, simultaneously with changes of cholate symmetric ν(COO) band (Figure 4c and e), together with only a moderate decrease of intensity of the 18C6 bands at 964 and 1107 cm^{-1} (Figure 4a and b). This is in accordance with the DSC result of obtained polymorphic phase transition at 380 K (Table 1 and Figure 1c). A sudden shift toward the lower wavenumbers of both antisymmetric and symmetric ν(COO) bands is observed around 380 K. This is accompanied by increase of the intensity of antisymmetric band (Figure 4d) and moderate decrease of the symmetric band intensity (Figure 4e). The observations show that one of the water molecules is hydrogen-bonded to the 18C6 moiety, while another is in slightly stronger interaction with carboxylic group of cholate anion. Increase of the ν_{as}(COO) band intensity indicates

Table 2. Assignment of Infrared Spectra of the 18C6·NaCh Complex at Room Temperature

18C6·NaCh	assignment
3457	water
3405	18C6
3289	unspecified ν(CH)
2972	unspecified ν(CH)
2938	unspecified ν(CH)
2913	18C6
2864	18C6
2824	18C6
1656	ν(COO···H_2O)
1578	antisymmetric ν(COO)
1473	18C6
1432	18C6
1406	symmetric ν(COO)
1351	18C6
1320	cholate
1292	18C6
1280	18C6
1268	cholate
1250	18C6
1227	unspecified alkyl
1205	cholate
1107	18C6
1082	unspecified alkyl
1045	cholate
985	cholate
965	18C6
837	18C6
785	
750	
712	
614	
590	18C6
528	18C6
475	18C6

an increasing ionic character of the bonding between Na^+ and carboxylate moiety of cholate, caused by release of hydrogen bonded water molecule. Difference of the ν_{as}(COO) and ν_s(COO) band positions indicate monodentate bonding over the whole temperature range. The most significant change occurs around 380 K, when for the symmetric band shift of $\Delta\nu_s$ = 15 cm^{-1} is observed, while for antisymmetric band no shift is resolved in the spectra. This gives the change in mutual distance between antisymmetric and symmetric band from 172 to 185 cm^{-1}. This transition obviously corresponds to change in bonding due to the dehydration and partial decomplexation of 18C6. However, TG does not show a significant decrease of the mass, which indicates that decomplexed 18C6 mainly remains in the sample. Decomplexation of 18C6 from NaCh·18C6 is also confirmed by comparison of IR spectra of the sample as obtained above 400 K with spectrum of purchased NaCh (see Supporting Information, Figure S2).

It is clear also from PXRD results (Figure 2d) that crystalline 18C6·NaCh complex suffers two phase changes, accompanied by dehydration. The RT phase (Figures 2d and 5, Table 3) has been indexed to a triclinic lattice. It is already known that the cholic acid molecule crystallizes in orthorhombic system in a kind of crossing structure.[58] The intercalation of such a molecule into the 18-crown-6 cavity changes the type of crystal system, and

dx.doi.org/10.1021/la501155s | Langmuir 2014, 30, 6274−6285

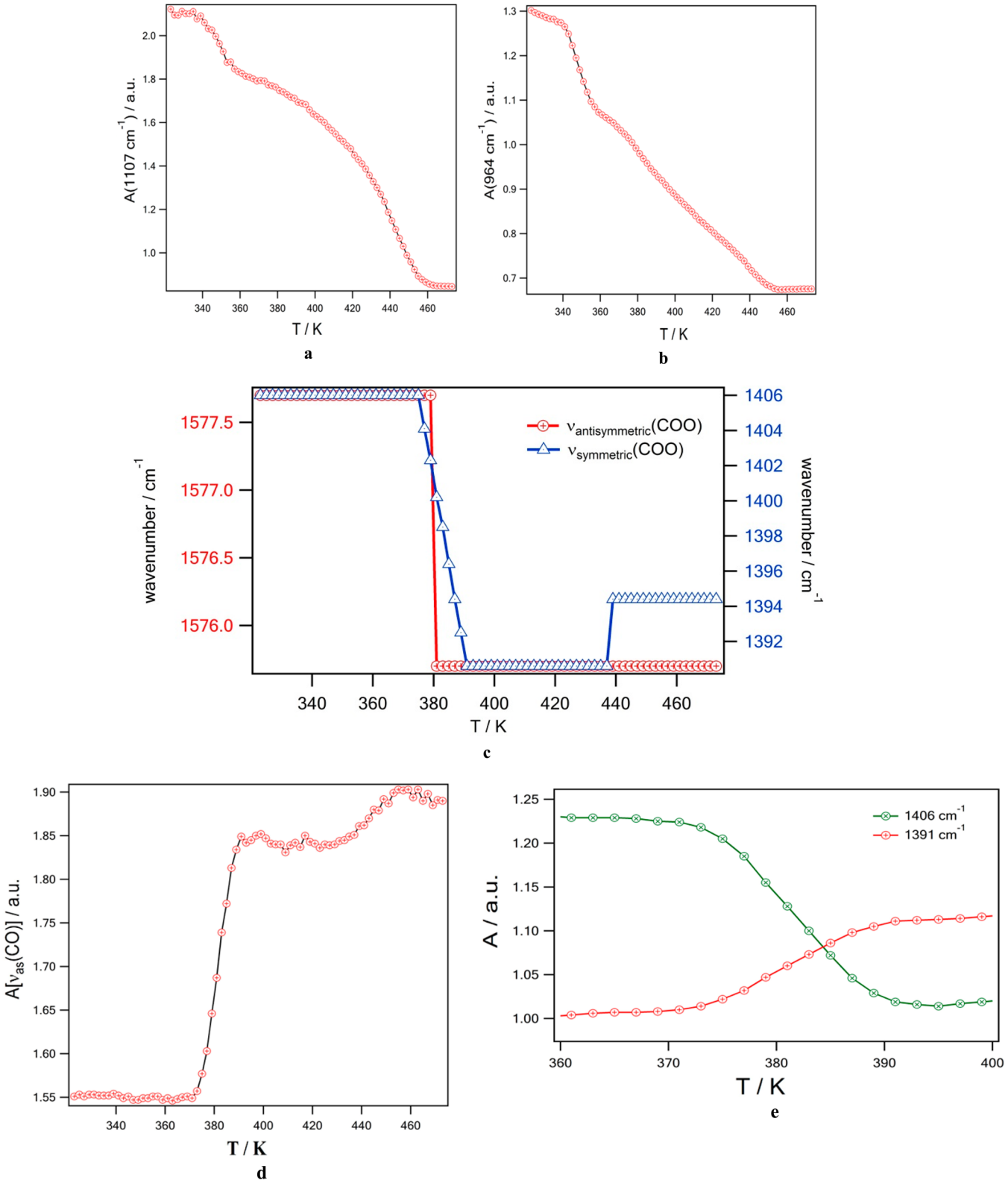

Figure 4. Temperature dependence of the absorption of the features due to the 18C6 crown for examined compound: 1107 cm^{-1} band (a); 964 cm^{-1} band (b). Temperature dependence of the antisymmetric and symmetric ν(COO) peak position (c) and absorption of antisymmetric ν(COO) band (d); absorptions of symmetric ν(COO) band (e).

consequently causes the elongation of the *a* and *c* axes, and shortening of the *b* axis of the crystal lattice (Table 3). According to the results, the complex exhibits two polymorphic transitions, both occurring simultaneously with dehydration of the sample, in accordance with other experimental results. The high temperature phases are monoclinic, as shown in Figures 6 and 7. As is evident from Table 3, lattice parameters of the two monoclinic phases are very close to each other, suggesting very similar

dx.doi.org/10.1021/la501155s | *Langmuir* 2014, 30, 6274−6285

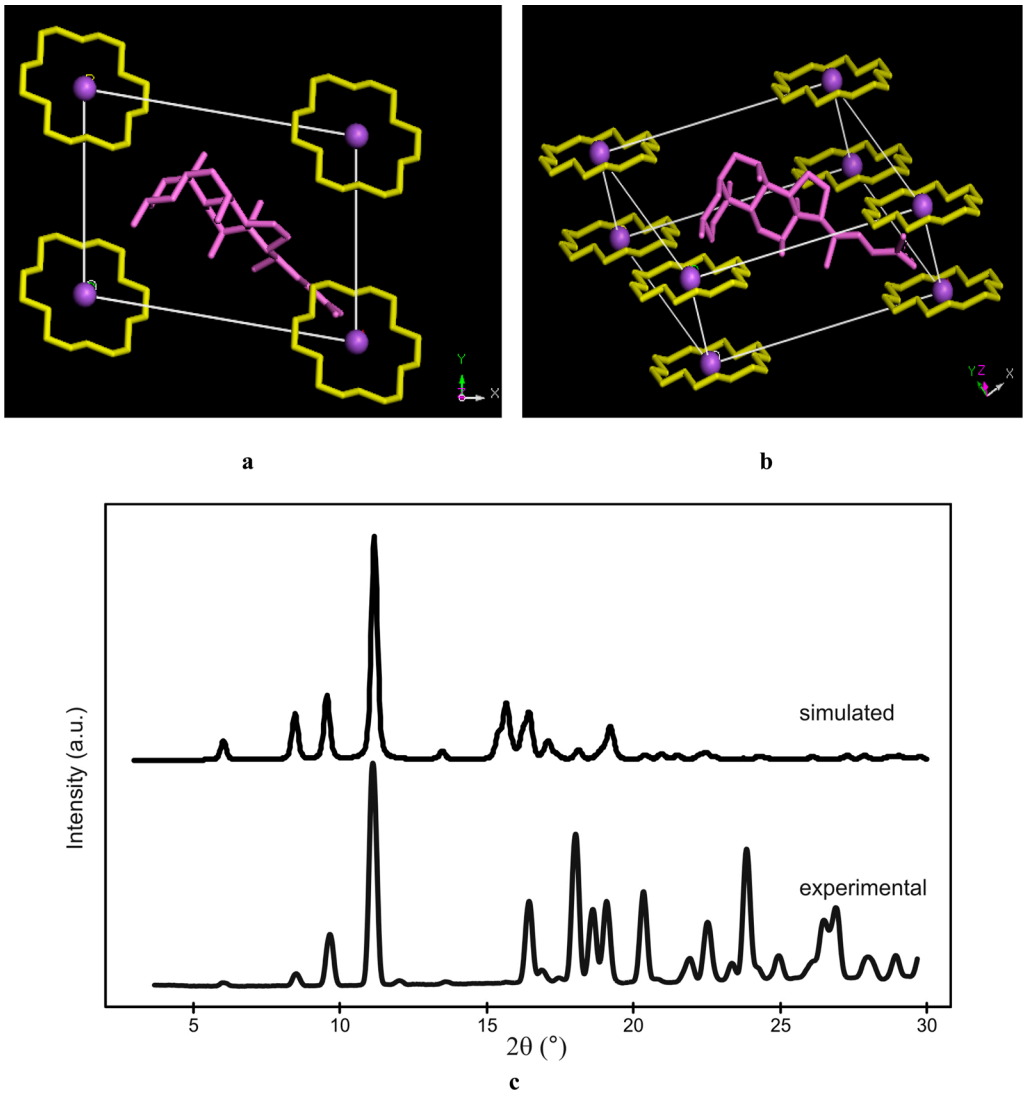

Figure 5. Molecular model of the room temperature phase of 18C6·NaCh; view along *c*-axis, (a) side view (b). The 18-crowns are colored yellow, while the cholic group is colored purple. For clarity, the hydrogen atoms are omitted. Experimental and simulated diffraction patterns of the room temperature phase of 18C6·NaCh (c).

Table 3. Lattice Parameters of Room Temperature Phase and Higher Temperature Phases of 18C6·NaCh, Determined by PXRD

		lattice parameters						
T/K	structure type	*a*/Å	*b*/Å	*c*/Å	*α*/deg	*β*/deg	*γ*/deg	*V*/Å^3
273	triclinic, *P*1	15.45	10.60	6.84	91.7	105.6	98.6	1063.9
363	monoclinic, *P*2	12.25	12.65	8.26	90.0	90.0	107.9	1218.0
390	monoclinic, *P*2	12.16	11.60	8.20	90.0	90.0	103.0	1127.0

structure. According to the quantum chemistry studies, this could be due to the changes of minimum energy 18C6−Na^+ conformers.[4]

To construct the structural models of the three phases, diffraction patterns for proposed models were simulated and compared to those obtained by experiment. Figures 5−7 show the models for which the best fit between simulated and experimental diffractograms has been achieved. PXRD diffractograms of 18C6·NaCh at different temperatures as well as indexing of room temperature phase and higher temperature phases of 18C6-NaCh are shown in Figure S3 and Table S1 in the Supporting Information. Having in mind the molecular mass of 18C6·NaCh, and assuming a density of 1.0 g cm^{-3}, the volume of the molecule can be estimated to be 1155 Å^3. Comparison of this with unit cell volume suggests for all three phases that there is only one molecule is the unit cell. As the molecule is chiral, no mirror or inverse center is possible in the structures. Thus, the space group of the triclinic phase can only be *P*1 (Figure 5), as it was obtained also for the 18C6−potassium picrate complex.[52] Formation of different host frameworks and network patterns within cholic acid compounds[39−43] seems to be very common. Cholic acid and *n*-alkylammonia form bilayer-like structures in the monoclinic phase, sandwich-type structure for 1:1 complexes, and crossing-type bilayers for 2:1 complexes.[42] It seems that, in this case, the arrangement in the triclinic phase also appears as layerlike, with the crown ether unit and sodium on one side, and

dx.doi.org/10.1021/la501155s | *Langmuir* 2014, 30, 6274−6285

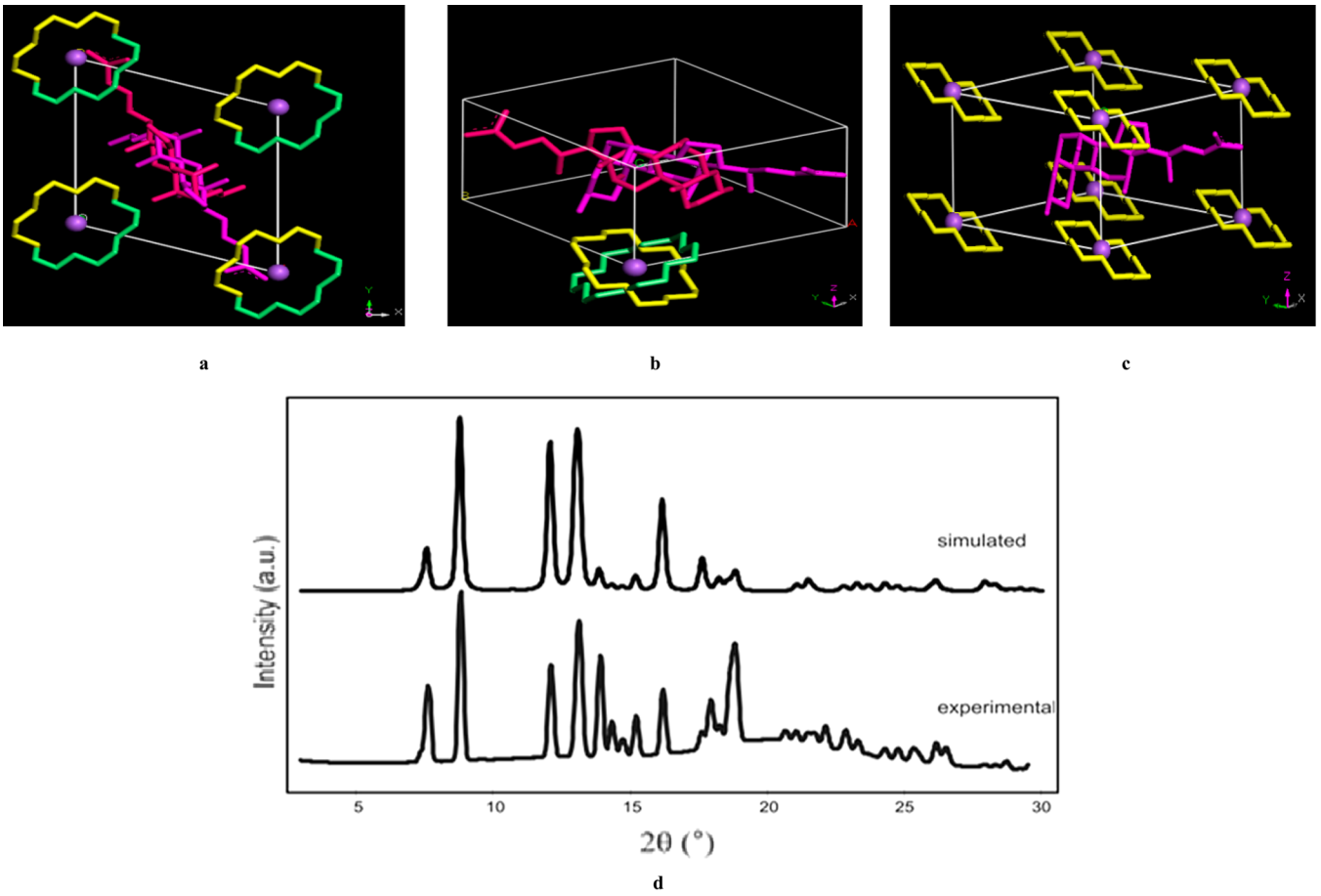

Figure 6. Molecular model of the medium temperature phase of 18C6·NaCh at 363 K: view along *c*-axis (a), side view (b, c). The 18-crowns are colored yellow and green, while the cholic group is colored purple and magenta. For clarity, hydrogen atoms are omitted. The model before the application of the 2-fold rotational symmetry along *c*-axis (c). Experimental and simulated diffraction patterns of 18C6·NaCh at 363 K (d).

the cholate anion on the other side, similar to that found for 18C6−sodium 4-(1-pentylheptyl)benzenesulfonate.[56] Unlike these results, the crystal smectic phase layers of 18C6−sodium *n*-dodecyl sulfate are composed of repetitive units of two crown ether layers with extended dodecyl chains.[56] For the two monoclinic phases (Figures 6 and 7), the fact that there exists a unique axis requires it to be a 2-fold axis, so the space group can only be assigned as *P*2. In addition, as there is only one molecule in the unit cell and the molecule itself do not have a 2-fold rotational axis, we propose that the 2-fold symmetry originates from the molecules taking randomly one of the two different configurations, so-called "orientational disorder" (related by a 2-fold symmetry) in the unit cell. This may also explain the diffuse scattering observed around $2\theta = 22°$ for the two monoclinic phases.

Liquid-like State Phase Transitions. Thermogravimetric analysis (Figure 2a) shows that the most prominent decrease in mass for this system occurs between 423 and 523 K, with the transition temperature (inflection point of TG for the mass decrease in the defined temperature period) of 493 K. The decrease in mass of the sample in the considered step with respect to starting mass m_0 was 0.37, which is undoubtedly attributed to decomplexation with consequent evaporation of free 18C6 from sample. The transition temperatures and thermodynamic parameters given by the DSC together with the thermodynamic parameters for decomplexation, calculated from the absorbance measurement of complexed and decomplexed sodium salt (IR), explained in the "Thermodynamics of the 18C6-Crown Decomplexation" subsection, are shown in Table 1. Temperature-dependent infrared spectroscopy was used in order to explain the thermal changes on the molecular level for this temperature period (Figures 1c, 3, and 4).

IR spectra in Figure 4e show an isosbestic point at 1395 cm^{-1}, which indicates simple equilibrium between the NaCh·18C6 complex and NaCh. Above 400 K, the area of the ν(OH) region remains constant, reflecting that the sample is completely dehydrated and the absorbance in this region is exclusively due to the cholate OH groups. Microscopic observations detected at 400 K characteristic patterns of chiral nematic (cholesteric) − partly homeotropic, partly $s = 1$ disclinations, with dark patches that indicate helix, that is, chirality (Figure 1d), but the texture starts to disappear due to partial decomposition, which is in accordance with previously mentioned IR results. Thermal properties of 18C6·NaCh complex are very similar to those obtained for 18C6-sodium *n*-dodecylsulfate and 18C6-sodium 4-(1-pentylheptyl)benzenesulfonate.[56] The formation of liquid crystalline phases is very common in complexes with crown ethers, but unlike the examined one most of the mesophases formed are stable until isotropization and are enantiotropic.[45−51] Unlike chiral nematic behavior noticed in the examined complex, smectic phases were obtained for other 18C6 complexes,[56] hexagonal columnar mesophases are formed in gallic acid substituted *ortho*-terphenyl dimers linked by a central 18C6 ether[40] or dibenzo 18C6 with different alkyl chain lengths,[46] and

dx.doi.org/10.1021/la501155s | *Langmuir* 2014, 30, 6274−6285

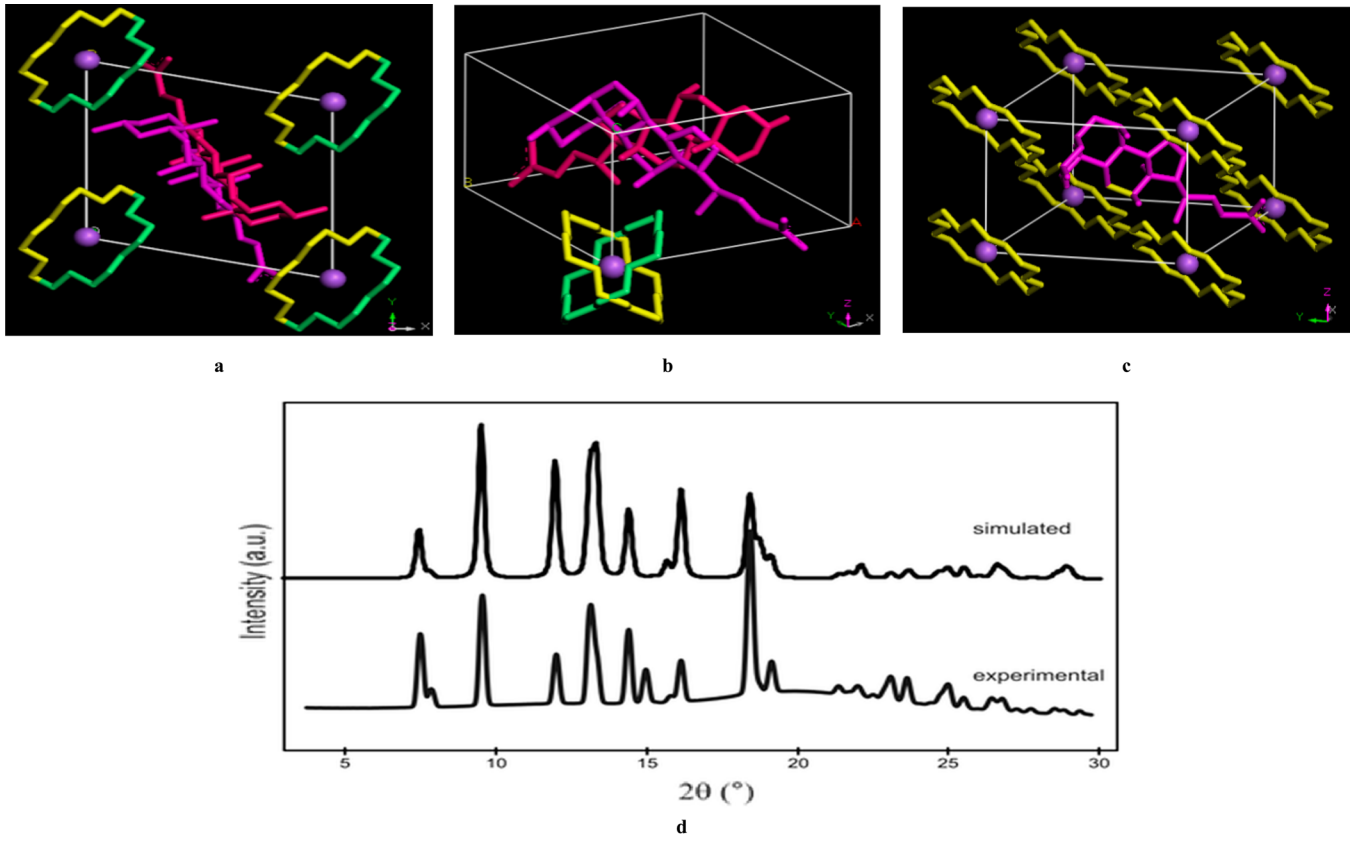

Figure 7. Molecular model of the high temperature phase of 18C6·NaCh at 390 K: view along *c*-axis (a) and side view (b, c). The 18-crowns are colored yellow and green, while the cholic group is colored purple and magenta. For clarity, hydrogen atoms are omitted. Only the model before the application of the 2-fold rotational symmetry along *c*-axis is shown in (c). Experimental and simulated diffraction patterns of 18C6·NaCh at 390 K (d).

nematic liquid crystals as well as smectic A phase in combination of 18C6 or rodlike 4,4″ didecyloxypterphenyl unit.[56] The diversity in thermal and thermotropic behavior of 18C6 complexes points to the promoting effect of the attached groups or guest molecules in the complex.

The partial decomposition also matches with the result of temperature dependence of the IR baseline absorption at 2500 cm^{-1}, shown in Figure 3c. The slow decomplexation is seen as an abrupt increase of absorbance above 395 K, with a transition temperature at 445 K, as determined by differentiation. In this range, a simultaneous decrease of the absorption at 1107, 964, and 837 cm^{-1} (Figure 4a and b) indicates the release of 18C6 from the sample. However, it should be mentioned that the IR baseline behaves different from that of TG, indicating significantly lower transition temperatures. However, this is not surprising, since the two techniques reflect different processes. Namely, the variation of IR baseline absorption is due to decomplexation of the 18C6 from Na^+. On the other hand, TG reflects evaporation of the free 18C6 from the sample. The intensities of IR features due to 18C6 vibrations are much better correlated with TG.

A steeper drop of the intensities of all IR spectral features due to the 18C6 moiety above 410 K is well correlated with TG, and is explained by evaporation of free crown 18C6 from the sample, which is now of liquid-like appearance. The difference in the shapes of curves is a result of the different oscillators, which cause these bands. The band at 1107 cm^{-1} is due to the ν(C−O) of crown ether. Thus, the change in absorption occurs due both to decomplexation and diffusion, resulting in nonlinear dependence. On the other hand, the band at 964 cm^{-1} is assigned to ν(C−O−C) and is only slightly affected by complexation. Thus, its decrease reflects only diffusion of crown 18C6 from the system, resulting in linear dependence. Obviously, diffusion in the liquid phase is significantly facilitated by transition to liquid phase. After that, a moderate change in the symmetric band position, accompanied by increase of both symmetric and antisymmetric ν(COO) band intensity, occurs at 440 K, which coincides to transition between liquid crystal to disordered liquid phase (isotropization) with simultaneous but complete decomposition (Table 1).

4. CONCLUSIONS

A compound constituting of 18C6 ether and NaCh surfactant was synthesized as a 1:1 coordination complex, and its structure was confirmed with elemental analysis and NMR spectroscopy. Its thermal behavior was examined by the techniques that were of great complementarity. Thermogravimetric and differential thermal analysis, differential scanning calorimetry, temperature-dependent IR spectroscopy, PXRD, and microscopic observations gave a detailed insight about phase transitions of the complex. Temperature dependent IR spectroscopy and PXRD solved the problem on the molecular level and gave a detailed view of the microscopic background of macroscopically observable phase transitions. The structure during thermal treatment was observed with powder XRD, and molecular models of the phases were made. Very good fit is achieved between the experimental and calculated values of the diffraction angles, and the molecular models presented are results of tedious trial-and-error work to get intensity matching. Considering the low symmetry (triclinic and monoclinic) and powder diffraction, this

dx.doi.org/10.1021/la501155s | *Langmuir* 2014, 30, 6274−6285

gave very valuable information on the changes of ordering during the solid-state phase transitions.

The 18C6·NaCh complex shows complex thermal behavior. Dehydration of the sample is a two-step process, occurring at 350 and 380 K. The two water molecules are absorbed to each formula unit, where the first is hydrogen bonded to the 18C6 ligand and another to the carboxylic group of the cholate anion. The complex goes through two solid−solid polymorphic transitions, accompanied by dehydration. The room temperature phase is indexed to a triclinic lattice with the *P*1 space group, while the high temperature phases are monoclinic with the *P*2 space group, and there is only 1 molecule in the unit cell. The lattice parameters of the two monoclinic phases are very similar to each other, suggesting that their structure is also very similar. The molecules take randomly one of the two different configurations in the unit cell, resulting in the 2-fold symmetry.

The formation of the liquid crystalline phase seen through characteristic patterns of cholesteric phase occurs simultaneously with partial decomposition. This process is followed by the complete decomplexation of the Na^+ ion from the crown 18C6 ligand and consequent diffusion of the crown 18C6 from the sample, seen as an abrupt increase of absorbance in the IR spectra above 395 K, with a transition temperature at 445 K. The study provides the relationship between molecular structure, thermal properties, and stability of the complex. We hope this work will be useful for the previously mentioned potentional applications of these new and similar synthesized crown complexes.

■ ASSOCIATED CONTENT

Ⓢ Supporting Information

IR spectra of the 18C6·NaCh complex in the 3700−3180 cm^{-1} range, taken at different temperatures; comparison of the room temperature IR spectrum of purchased sodium cholate (NaCh) and of the 18C6·NaCh high temperature phase; PXRD diffractograms of 18C6·NaCh at different temperatures; indexing of room temperature phase and higher temperature phases of 18C6·NaCh. This material is available free of charge via the Internet at http://pubs.acs.org.

■ AUTHOR INFORMATION

Corresponding Authors

*E-mail: tmihelj@irb.hr. Fax: +38514680245. Tel: +38514571211.
*E-mail: vlastom@irb.hr.

Notes

The authors declare no competing financial interest.

■ ACKNOWLEDGMENTS

This work has received support from the Ministry of Education, Science and Sport of the Republic of Croatia (Projects No. 098-0982915-2949, 098-0982904-2941). The authors are grateful to Prof. Dr. Sc. G. Ungar and Dr. Sc. Xiangbing Zeng, Department of Materials Science and Engineering, University of Sheffield, for the PXRD measurements and interpretation of the obtained diffractograms.

■ REFERENCES

(1) Gámez, F.; Hurtado, P.; Martínez−Haya, B.; Berden, G.; Oomens, J. Vibrational Study of Isolated 18-Crown-6 Ether Complexes with Alkaline-Earth Metal Cations. *Int. J. Mass spectrom.* **2011**, *308*, 217−224.
(2) Izatt, R. M.; Pawlak, K.; Bradshaw, J. S.; Bruening, R. L. Thermodynamic and Kinetic Data for Macrocycle Interactions with Cations and Anions. *Chem. Rev.* **1991**, *91*, 1721−2085.
(3) Markova, N. V.; Vasiliev, V. P. Thermochemistry of 18C6 Complexation with Alkali, Alkaline Earth Metal Cations and Ammonium Ion. *J. Therm. Anal.* **1995**, *45*, 695−701.
(4) De, S. Preferential Interaction of Charged Alkali Metal Ions (guest) within a Narrow Cavity of Cyclic Crown Ethers (neutral Host): A Quantum Chemical Investigation. *J. Mol. Struct.* **2010**, *941*, 90−101.
(5) Anderson, J.; Paulsen, E. S.; Dearden, D. V. Alkali Metal Binding Energies of Dibenzo-18-Crown-6: Experimental and Computational Results. *Int. J. Mass Spectrom.* **2003**, *227*, 63−76.
(6) Doxsee, K. M.; Francis, P. E.; Weakley, T. J. R. Hydration, Ion Pairing, and Sandwich Motifs in Ammonium Nitrate Complexes of Crown Ethers. *Tetrahedron* **2000**, *56*, 6683−6691.
(7) Hurtado, P.; Hortal, A. R.; Gámez, F.; Hamad, S.; Martínez-Haya, B. Gas-Phase Complexes of Cyclic and Linear Polyethers with Alkali Cations. *Phys. Chem. Chem. Phys.* **2010**, *12*, 13752−13758.
(8) Martínez-Haya, B.; Hurtado, P.; Hortal, A. R.; Hamad, S.; D. Steill, J.; Oomens, J. Emergence of Symmetry and Chirality in Crown Ether Complexes with Alkali Metal Cations. *J. Phys. Chem. A* **2010**, *114*, 7048−7054.
(9) Peiris, D. M.; Yang, Y.; Ramanathan, R.; Williams, K. R.; Watson, C. H.; Eyler, J. R. Infrared Multiphoton Dissociation of Electrosprayed Crown Ether Complexes. *Int. J. Mass Spectrom. Ion Phys.* **1996**, *157−158*, 365−378.
(10) Pedersen, C. J. Cyclic Polyethers and Their Complexes with Metal Salts. *J. Am. Chem. Soc.* **1967**, *89*, 7017−7036.
(11) Raevsky, O. A.; Solov'ev, V. P.; Solotnov, A. F.; Schneider, H.-J.; Rüdiger, V. Conformation of 18-Crown-5 and Its Influence on Complexation with Alkali and Ammonium Cations: Why 18-Crown-5 Binds More Than 1000 Times Weaker Than 18C6. *J. Org. Chem.* **1996**, *61*, 8113−8116.
(12) Cram, D. Synthetic Host-Guest Chemistry. In *Applications of Biochemical Systems in Organic Chemistry*; Bryan, J., Sih, C. J., Perlman, D., Eds; Wiley: New York, 1976; Vol. *10*, p 815.
(13) Vögtle, F.; Weber, E. *Host Guest Complex Chemistry: Macrocycles: Synthesis, Structures, Applications*; Springer: New York, 1985.
(14) Unruh, G.; Cumbest, J. Crown Ethers Enhance Ionic Residue Removal. *Res. Dev.* **1994**, 1−5.
(15) Moyer, B. A.; Birdwell, J. F.; Bonnesen, P. V.; Delmau, L. H. Use of Macrocycles in Nuclear-Waste Cleanup: A Realworld Application of a Calixcrown in Cesium Separation Technology. In *Macrocyclic Chemistry*; Gloe, K., Ed.; Springer-Verlag: Berlin/Heidelberg; pp 383−405.
(16) Darwish, I. A.; Uchegbu, I. F. The Evaluation of Crown Ether Based Niosomes as Cation Containing and Cation Sensitive Drug Delivery Systems. *Int. J. Pharm.* **1997**, *159*, 207−213.
(17) Muzzalupo, R.; Nicoletta, F. P.; Trombino, S.; Cassano, R.; Iemma, F.; Picci, N. A New Crown Ether as Vesicular Carrier for 5-Fluoruracil: Synthesis, Characterization and Drug Delivery Evaluation. *Colloids Surf., B* **2007**, *58*, 197−202.
(18) Gokel, G. W.; Durst, H. D. Crown Ether Chemistry: Principles and Applications. *Aldrichimica Acta* **1976**, *9*, 3−12.
(19) Bereczki, R.; Ágai, B.; Bitter, I. Synthesis and Alkali Cation Extraction Ability of New Mono and Bis(benzocrown Ether)s with Terminal Alkenyl Groups. *J. Inclusion Phenom.* **2003**, *47*, 53−58.
(20) Nakajima, M.; Kimura, K.; Shono, T. Liquid Chromatography of Alkali and Alkaline Earth Metal Salts on Poly(benzo-15-Crown-5)- and Bis(benzo-15-Crown-5)-Modified Silicas. *Anal. Chem.* **1983**, *55*, 463−467.
(21) Jin, Y.; Fu, R.; Huang, Z. Use of Crown Ethers in Gas Chromatography. *J. Chromatogr. A* **1989**, *469*, 153−159.
(22) Wong, A.; Wu, G. Solid-State ^{23}Na Nuclear Magnetic Resonance of Sodium Complexes with Crown Ethers, Cryptands, and Naturally Occurring Antibiotic Ionophores: A Direct Probe to the Sodium-Binding Sites. *J. Phys. Chem. A* **2000**, *104*, 11844−11852.
(23) Koch, K. J.; Aggerholm, T.; Nanita, S. C.; Cooks, R. G. Clustering of Nucleobases with Alkali Metals Studied by Electrospray Ionization Tandem Mass Spectrometry: Implications for Mechanisms of Multi-strand DNA Stabilization. *J. Mass Spectrom.* **2002**, *37*, 676−686.

(24) Chaput, J. C.; Switzer, C. A DNA Pentaplex Incorporating Nucleobase Quintets. *Proc. Natl. Acad. Sci. U.S.A.* **1999**, *96*, 10614−10619.
(25) Kudo, Y.; Katsuta, S.; Takeda, Y. Potentiometric Determination of the Ion-Pair Formation Constant of a Univalent Cation-Neutral Ligand Complex with an Anion in Water Using an Ion-Selective Electrode. *Anal. Sci.* **1999**, *15*, 597−599.
(26) Hofmann, A. F. Bile Acids as Drugs: Principles, Mechanisms of Action and Formulations. *Ital J. Gastroenterol.* **1995**, *27*, 106−113.
(27) Berlati, F.; Ceschel, G.; Clerici, C.; Pellicciari, R.; Roda, A.; Ronchi, C. The Use of Bile Acids as Antiviral Agents. Patent WO 9400126, 1994.
(28) Marples, B.; Stretton, R. Use of Steroidal Compounds as Anti-Fungal Agents. Patent WO 9013298, 1990.
(29) Savage, P. B.; Li, C.; Taotafa, U.; Ding, B.; Guan, Q. Antibacterial Properties of Cationic Steroid Antibiotics. *FEMS Microbiol. Lett.* **2002**, *217*, 1−7.
(30) Davis, A. P.; Joos, J.-B. Steroids as Organising Elements in Anion Receptors. *Coord. Chem. Rev.* **2003**, *240*, 143−156.
(31) Nath, S.; Maitra, U. A Simple and General Strategy for the Design of Fluorescent Cation Sensor Beads. *Org. Lett.* **2006**, *8*, 3239−3242.
(32) Soto Tellini, V. H.; Jover, A.; Meijide, F.; Vázquez Tato, J.; Galantini, L.; Pavel, N. V. Supramolecular Structures Generated by a P-Tert-Butylphenyl-Amide Derivative of Cholic Acid: From Vesicles to Molecular Tubes. *Adv. Mater.* **2007**, *19*, 1752−1756.
(33) Yoshii, M.; Yamamura, M.; Satake, A.; Kobuke, Y. Supramolecular Ion Channels from a Transmembrane Bischolic Acid Derivative Showing Two Discrete Conductances. *Org. Biomol. Chem.* **2004**, *2*, 2619−2623.
(34) Judd, L. W.; Davis, A. P. From Cholapod to Cholaphane Transmembrane Anion Carriers: Accelerated Transport through Binding Site Enclosure. *Chem. Commun.* **2010**, *46*, 2227−2229.
(35) Bonar-Law, R. P.; Mackay, L. G.; Sanders, J. K. M. Morphine Recognition by a Porphyrin−cyclocholate Molecular Bowl. *J. Chem. Soc., Chem. Commun.* **1993**, 456−458.
(36) Balasubramanian, R.; Maitra, U. Design and Synthesis of Novel Chiral Dendritic Species Derived from Bile Acids. *J. Org. Chem.* **2001**, *66*, 3035−3040.
(37) Maitra, U.; Balasubramanian, S. Design and Synthesis of New Bile Acid-Based Macrocycles. *J. Chem. Soc., Perkin Trans. 1* **1995**, 83−88.
(38) Nakano, K.; Mochizuki, E.; Yasui, N.; Morioka, K.; Yamauchi, Y.; Kanehisa, N.; Kai, Y.; Yoswathananont, N.; Tohnai, N.; Sada, K.; et al. Mechanism of Selective and Unselective Enclathration by a Host Compound Possessing Open, Flexible Host Frameworks. *Eur. J. Org. Chem.* **2003**, *2003*, 2428−2436.
(39) Nakano, K.; Sada, K.; Kurozumi, Y.; Miyata, M. Importance of Packing Coefficients of Host Cavities in the Isomerization of Open Host Frameworks: Guest-Size-Dependent Isomerization in Cholic Acid Inclusion Crystals with Monosubstituted Benzenes. *Chem.—Eur. J.* **2001**, *7*, 209−220.
(40) Miyata, M.; Sada, K. Deoxycholic Acid and Related Hosts. In *Comprehensive Supramolecular Chemistry*; Atwood, J. L., Davies, J., McNicol, D., Lehn, J., Toda, F., Bishop, R., Eds.; Pergamon: Oxford, 1966; Vol. *6*, pp 147−176.
(41) Valkonen, A.; Lahtinen, M.; Tamminen, J.; Kolehmainen, E. Solid State Structural Studies of Five Bile Acid Derivatives. *J. Mol. Struct.* **2008**, *886*, 197−206.
(42) Tomašić, V.; Štefanić, Z. Cholic Acid as Host for Long Linear Molecules: A Series of Co-Crystals with N-Alkylammonia. *CrystEngComm* **2007**, *9*, 1124−1128.
(43) Miyata, M.; Tohnai, N.; Hisaki, I. Supramolecular Chirality in Crystalline Assemblies of Bile Acids and Their Derivatives; Three-Axial, Tilt, Helical, and Bundle Chirality. *Molecules* **2007**, *12*, 1973−2000.
(44) Kato, K.; Tohnai, N.; Miyata, M. Hierarchical Prediction Process of Cholic Acid Crystal Structures Based on Characteristic Helical Assemblies. *Mol. Cryst. Liq. Cryst.* **2005**, *440*, 125−132.
(45) Steinke, N.; Kaller, M.; Nimtz, M.; Baro, A.; Laschat, S. Columnar Liquid Crystals Derived from Crown Ethers with Two Lateral Ester-Substituted Ortho-Terphenyl Units: Unexpected Destabilisation of the Mesophase by Potassium Iodide. *Liq. Cryst.* **2010**, *37*, 1139−1149.
(46) Schultz, A.; Laschat, S.; Saipa, A.; Gießelmann, F.; Nimtz, M.; Schulte, J. L.; Baro, A.; Miehlich, B. Columnar Liquid Crystals with a Central Crown Ether Unit. *Adv. Funct. Mater.* **2004**, *14*, 163−168.
(47) Nagvekar, D. S.; Delaviz, Y.; Prasad, A.; Merola, J. S.; Marand, H.; Gibson, H. W. Synthesis and Properties of Cholesteryl Esters Bearing 32- and 16-Membered Crown Ethers. *J. Org. Chem.* **1996**, *61*, 1211−1218.
(48) Goodby, J.; Mehl, G.; Saez, I.; Tuffin, R.; Mackenzie, G.; Auzelyvelty, R.; Benvegnu, T.; Plusquellec, D. Liquid Crystals with Restricted Molecular Topologies: Supermolecules and Supramolecular Assemblies. *Chem. Inform.* **1998**, *29*, 2057−2070.
(49) Leblanc, K.; Berdagué, P.; Rault, J.; Bayle, J.-P.; Judeinstein, P. Synthesis and Ionic Properties of Nematic Compounds Bearing an Ether-Crown Moiety: An NMR Approach. *Chem. Commun.* **2000**, 1291−1292.
(50) Nishikawa, Y.; Watanabe, T.; Yoshida, H.; Ikeda, M. Phase Transition Behaviors of Crown-Ether Derivative and Its Sodium Ion Complex. *Thermochim. Acta* **2005**, *431*, 81−86.
(51) He, G. X.; Wada, F.; Kikukawa, K.; Shinkai, S.; Matsuda, T. Syntheses and Thermal Properties of New Liquid Crystals Bearing a Crown Ether Ring: Cation Binding in the Nematic Phase. *J. Org. Chem.* **1990**, *55*, 541−548.
(52) Barnes, J.; Collard, J. 18-Crown-6−Potassium Picrate (1/1). *Acta Crystallogr., Sect. C: Cryst. Struct. Commun.* **1988**, *44*, 565−566.
(53) Ahonen, K. V.; Lahtinen, M. K.; Löfman, M. S.; Kiesilä, A. M.; Valkonen, A. M.; Sievänen, E. I.; Nonappa; Kolehmainen, E. T. Structural Studies of Five Novel Bile Acid-4-Aminopyridine Conjugates. *Steroids* **2012**, *77*, 1141−1151.
(54) Meijide, F.; Trillo, J. V.; Frutos, S. de; Galantini, L.; Pavel, N. V.; Soto, V. H.; Jover, A.; Tato, J. V. Crystal Structure of Head-to-Head Dimers of Cholic and Deoxycholic Acid Derivatives with Different Symmetric Bridges. *Steroids* **2013**, *78*, 247−254.
(55) Zimmermann, B.; Baranović, G. Determination of Phase Transition Temperatures by the Analysis of Baseline Variations in Transmittance Infrared Spectroscopy. *Appl. Spectrosc.* **2009**, *63*, 1152−1161.
(56) Mihelj, T.; Tomašić, V.; Biliškov, N.; Liu, F. Temperature-Dependent IR Spectroscopic and Structural Study of 18-Crown-6 Chelating Ligand in the Complexation with Sodium Surfactant Salts and Potassium Picrate. *Spectrochim. Acta, Part A* **2014**, *124*, 12−20.
(57) Tomašić, V.; Biliškov, N.; Mihelj, T.; Štefanić, Z. Thermal Behaviour and Structural Properties of surfactant—Picrate Compounds: The Effect of the Ammonium Headgroup Number. *Thermochim. Acta* **2013**, *569*, 25−35.
(58) Miki, K.; Kasai, N.; Shibakami, M.; Chirachanchai, S.; Takemoto, K.; Miyata, M. Crystal Structure of Cholic Acid with No Guest Molecules. *Acta Crystallogr., Sect. C: Cryst. Struct. Commun.* **1990**, *46*, 2442−2445.